

**INVESTIGATING THE EFFECTS OF CD40-CD40 LIGAND ON
ACTIVATED B CELL DIFFUSE LARGE B CELL LYMPHOMA B
CELL RECEPTOR SIGNALING**

A Dissertation
Presented to
The Academic Faculty

by

Deepali Balasubramani

In Partial Fulfillment
of the Requirements for the Degree
Master of Science in the
School of Biomedical Engineering

Georgia Institute of Technology and Emory University
May 2022

COPYRIGHT © 2022 BY DEEPALI BALASUBRAMANI

**INVESTIGATING THE EFFECTS OF CD40-CD40 LIGAND ON
ACTIVATED B CELL DIFFUSE LARGE B CELL LYMPHOMA B
CELL RECEPTOR SIGNALING**

Approved by:

Dr. Ankur Singh
Wallace H. Coulter School of Biomedical
Engineering
Georgia Institute of Technology

Dr. Cheng Zhu
Wallace H. Coulter School of Biomedical
Engineering
Georgia Institute of Technology

Dr. Jean Koff
Department of Hematology and Medical
Oncology
Emory University School of Medicine

Dr. Ahmet Coskun
Wallace H. Coulter School of Biomedical
Engineering
Georgia Institute of Technology

Date Approved: 29 April 2022

ACKNOWLEDGEMENTS

Foremost I would like to express my sincere gratitude to Dr. Ankur Singh for giving me this research project opportunity and for his support and patience during my MS program. His ambition and drive encourage me to push my limits and grow as a scientist and engineer. I would also like to thank my committee members for their useful feedback and guidance.

I would also like to thank the Immunotherapy and Cellular Engineering Lab members for their constant support; in particular, I wish to recognize Grazia Marsico, Kristine Lai, Chris Carlson and Zhonghao Dai for their advice on technical matters and for their willingness to help whenever possible.

I would also like to thank my dear friends, Manya, Divya, Blanche, Moyo, Kingsley and Akshay, who inspired and motivated me to be persistent in achieving my goals. They were always ready to listen and share words of encouragement.

And finally, I would like to express my heartfelt gratitude to my siblings, Vrushali and Krishna and to my parents, Balasubramani and Kalavati, for their unconditional love, years of hard work and sacrifice and endless support.

TABLE OF CONTENTS

ACKNOWLEDGEMENTS	iii
LIST OF FIGURES	vi
LIST OF ABBREVIATIONS	viii
SUMMARY	ix
CHAPTER 1: INTRODUCTION	1
1.1 Diffuse Large B Cell Lymphoma	1
1.2 BCR Signaling Pathway	2
1.3 Lymphoid Tumor Microenvironment	4
1.4 B Cell Receptor Signaling and the Actin Cytoskeleton Coordination	5
1.5 Motivation and Objectives	6
CHAPTER 2: METHODS	7
2.1 Polymer and Peptides	7
2.2 Cell culture	7
2.3 DLBCL Lymphoma 2D model preparation	7
2.4 2D cell culture immunostaining	8
2.5 Organoid Fabrication	9
2.6 Organoid Immunostaining for Imaging	10
2.7 Confocal Imaging and Image analysis	11
2.8 Statistical analysis	11
CHAPTER 3: RESULTS	12
3.1 Comparison of different modes of antigen presentation in 2D and 3D ABD DLBCL models	12
3.2 Investigating CD40-CD40L effects on DLBCL BCR signaling in 2D vs 3D model	13
3.3 Investigating CD40-CD40L effects on DLBCL BCR signaling in 3D model	15
3.3.1 Actin expression and cell spreading with antigen and CD40L presentation in 3D model	16
3.3.2 CD40 cluster and expression with antigen and CD40L presentation in 3D model	18

3.3.3 BCR clustering and expression with antigen and CD40L presentation in 3D model	21
3.3.4 Colocalization analysis of IgM BCR, Actin and CD40	23
CHAPTER 4: DISCUSSION	26
CHAPTER 6: CONCLUSION AND FUTURE DIRECTIONS:	29
REFERENCES	30

LIST OF FIGURES

Figure 1: MYD88-TLR9-BCR signaling in ABC DLBCL	2
Figure 2: B Cell Receptor Signaling and the Actin Cytoskeleton Coordination	6
Figure 3: A) Organization of a lymph node. b) Schematic of our 3D model: Lymphoma Organoids. C) Schematic of our 2D model - Antigen/CD40L monolayer. All schematics generated using Biorender.	8
Figure 4: Schematic of lymphoma organoid formation and Michael Addition chemistry; organoids are encapsulated with lymphoma cells and follicular dendritic cells [25].	9
Figure 5: A) Cross section of ABC DLBCL CD3+ CD4+ OR CD8+ T cells(brown) and ABC DLBCLs(blue). B) Ly10 cells encapsulated in 7.5 wt% /vol organoids. (3D model) C) Ly10 cells spreading on 2D monolayer (2D model)	12
Figure 6: Cell spreading and filapodia formation in 2D cell culture (L) and 7.5 wt%/vol organoids (R).	13
Figure 7: A) Comparing fraction of cells with filapodia in 2D vs 3D. B) Comparing cell spreading area in 2D vs 3D	14
Figure 8: Comparing CD40 expression (A) and actin expression (B) in 2D vs 3D	15
Figure 9: Stiffness versus PEG-4MAL wt%/v	16
Figure 10: Comparing Actin MFI across three anti IgM/CD40L groups for each wt%/vol condition	16
Figure 11: Comparing Cell spreading MFI across three anti IgM/CD40L groups for each wt%/vol condition	17
Figure 12: A) Comparing normalized actin MFI with varying stiffness B) Comparing cell spreading area with varying stiffness	18
Figure 13: Comparing CD40 cluster number across three anti IgM/CD40L groups for each wt%/vol condition	19
Figure 14: Comparing CD40 MFI across three anti IgM/CD40L groups for each wt%/vol condition	19
Figure 15: A) Comparing normalized CD40 MFI with varying stiffness. B) Comparing CD40 cluster number with varying stiffness	20

Figure 16: Comparing IgM BCR Cluster number for each wt%/vol	21
Figure 17: Comparing IgM BCR MFI across three anti IgM/CD40L groups for each wt%/vol condition	21
Figure 18: A) Comparing nomalized IgM BCR MFI with varying stiffness. B) Comparing BCR Cluster number with varying stiffness	22
Figure 19: IgM BCR and CD40 cluster colocalization and Actin and CD40 colocalization observed in 12.5 wt%/vol organoids	23
Figure 20: IgM BCR and CD40 colocalization. Each point represents the average mander's overlap coefficient for each stack of an entire image file.	24
Figure 21: Actin and CD40 colocalization. Each point represents the average mander's overlap coefficient for each stack of an entire image file	25

LIST OF ABBREVIATIONS

ABC	Activated B Cell
AKT	Protein kinase B
ARP2/3	Actin Related Protein 2/3 complex
BLK	B-cell lymphocyte kinase
BLNK	B-cell linker protein
BTK	Bruton's tyrosine kinase
CAPZA	F-actin-capping protein subunit alpha
CD19	Cluster of Differentiation 19
CD40	Cluster of differentiation 40
CD40L	Cluster of differentiation 40 Ligand
CD79A	Cluster of differentiation CD79A
CD79B	Cluster of differentiation CD79B
DLBCL	Diffuse Large B Cell Lymphoma
ECM	Extracellular Matrix
FYN	Tyrosine-protein kinase Fyn
IgM BCR	Immunoglobulin M B Cell Receptor
ITAM	Immunoreceptor Tyrosine-Based Activation Motif
LAT2	Linker For Activation of T Cells Family Member 2
LYN	Tyrosine-protein kinase Lyn
LY-TME	Lymphoid Tumor Microenvironment
MAL	Maleimide
MAPK	Mitogen-activated protein kinase
MFI	Mean Fluorescence Intensity
MMP	Matrix metalloproteinases
MYD88	Myeloid differentiation primary response 88
NF-Kb	Nuclear factor kappa B
PEG	Poly (ethylene glycol)
PI3K	Phosphoinositide 3-kinase Rituximab, Cyclophosphamide, Doxorubicin, Vincristine, and Prednisone
R-CHOP	
SRC	Tyrosine-protein kinase Src
SYK	Tyrosine-protein kinase Syk
TLR-9	Toll-like Receptor 9
TRAF	Tumor necrosis factor receptor
VCAM	Vascular cell adhesion protein
WASP	Wiskott-Aldrich syndrome protein
WAVE	WASP-family verprolin-homologous protein

SUMMARY

Activated B cell-like diffuse large B-cell lymphoma (ABC-DLBCL), one of the more aggressive forms of non-Hodgkin lymphoma, accounts for one-third of all DLBCL cases. There is an urgent need to develop new therapeutic interventions, as 40% of patients either relapse after an initial response or do not respond to current therapies. B cell lymphomas depend on and interact with lymphoid tumor microenvironment (Ly-TME) cues such as immune cells, stromal cells, and the extracellular matrix, that contributes to their pathogenesis. Understanding the biophysical and cellular components Ly-TME and its impact on ABC BCR signaling is thus necessary for developing therapeutic interventions to improve clinical outcomes for ABC DLBCL patients. We aim to investigate the effects of Ly-TME cues, specifically CD4⁺ T cell signaling via CD40-ligand (CD40L) and extracellular matrix (ECM) stiffness on ABC BCR signaling. We synthesized 2D cell cultures (2D model) and lymphoma organoids (3D model) encapsulated with DLBCLs, soluble CD40L, and anti-IgM and varied organoid stiffness as well as antigen/CD40L presentation in both models. We observed B cell spreading and filopodia formation in both models, with enhanced B cell spreading and filopodia formation in the 2D models where membrane-bound antigen – B cell encounter was recapitulated. CD40-CD40L engagement reduced actin expression and cell spreading in the stiffer organoids, and CD40 and IgM BCR expression increased with increasing stiffness. Finally, we observed a significant effect of Ly-TME stiffness on colocalization of IgM BCR with CD40 and Actin, suggesting potential involvement of the ECM in promoting integrin expression and stimulating mechanotransduction pathways to contribute to the colocalization

CHAPTER 1: INTRODUCTION

1.1 Diffuse Large B Cell Lymphoma

Human lymphomas which include non-Hodgkin lymphomas such as Diffuse Large B Cell Lymphomas (DLBCL) encompass the 7th most frequently diagnosed form of human cancer [1,2]. The annual rate of new non-Hodgkin lymphoma cases was 19.6 per 100,000 men and women, and in 2018, approximately 743,176 people were living with non-Hodgkin lymphoma in the United States [1,2].

DLBCL is the most common form of NHL and is characterized by a diffuse proliferation of malignant B cells in lymph nodes and aggressive clinical behavior [3,4]. Gene expression profiling studies have revealed two molecular DLBCL subgroups: germinal center B cell-like (GCB), characterized by expression of genes typically expressed by normal B cells found in germinal centers, and activated B cell-like (ABC), characterized by NF- κ B activation [10] through B cell receptor (BCR) and toll-like receptor (TLR9) pathways [3,4]. ABC DLBCL, which is associated with a poor clinical prognosis, resembles plasmablasts that mark the transition between GC B cells and plasma cells [4].

Standard therapy for DLBCL includes combination chemoimmunotherapy with rituximab, cyclophosphamide, doxorubicin, vincristine, and prednisone (R-CHOP); however, 40% of patients either relapse after an initial response or do not respond to therapy [5]. B cell lymphomas depend on and interact with lymphoid tumor microenvironment (Ly- TME) cues such as immune cells, stromal cells, and the extracellular matrix, that contributes to their pathogenesis. Understanding the cellular and

biophysical cues in the lymphoid tumor microenvironment and its impact on BCR activation and signaling is thus necessary for developing therapeutic interventions to improve clinical outcomes for ABC DLBCL patients.

1.2 BCR Signaling Pathway

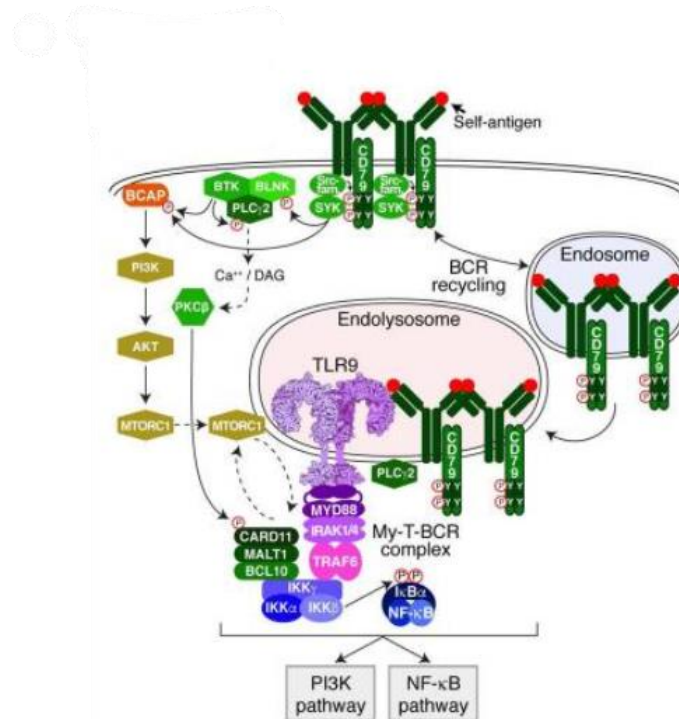


Figure 1: MYD88-TLR9-BCR signaling in ABC DLBCL

ABC DLBCL is highly dependent on constitutive NF-κB activation for survival. The nuclear factor-kappa B (NF-κB) transcription factor is involved in cellular processes associated with proliferation, cell death, development, as well as innate and adaptive immune responses. A complete BCR, transmembrane proteins located on outer surface of healthy and malignant B cell membrane, constitutes the antibody portion of the BCR that associates with a heterodimer of CD79A and CD79B [6]. Antigen engagement induces actin cytoskeleton reorganization, aggregation of BCR units and formation of signaling microclusters on the plasma membrane, resulting in phosphorylation of the

immunoreceptor tyrosine-based activation motif (ITAM) tyrosines present on the cytoplasmic tail of CD79A and CD79B by Src family kinases (SFKs) which include FYN, BLK and LYN [7]. SYK kinase can bind to phosphorylated ITAMs through the Src homology domains (SH2) [8] and is activated, resulting in the recruitment and activation of adapter proteins including BLNK, Bruton's tyrosine kinase (BTK), phosphatidylinositol 3-kinase (PI3K) and AKT [9]. Mutations affecting the ITAM motifs of CD79A and CD79B, collectively present in approximately 29% of ABC tumors, and kinases/adapter proteins result in oncogenic signaling [11].

Myeloid differentiation primary response 88 (MYD88), an adaptor protein and essential gene in ABC DLBCL [12], interacts with BCR and TLR9 to form the MyD88-TLR9-BCR (My-T-BCR) supercomplex (Figure 1) [3]. The My-T-BCR coordinates NF- κ B signaling by MYD88, Caspase Recruitment Domain Family Member 11 (CARD11), B-cell lymphoma/leukemia 10 (BCL10), and mucosa-associated lymphoid tissue lymphoma translocation protein 1 (MALT1) CBM complex, TRAF6, phosphorylated I κ B kinase (IKK) and NF- κ B transcription factor subunit p50 (NFKB1)[3]. The complex formation also involves internalization of Lamp1+ endolysosomes where the BCR can associate with TLR [3]. Understanding the effects of Ly-TME cues on BCR intracellular signaling proteins and kinases could contribute to the development of therapeutic interventions.

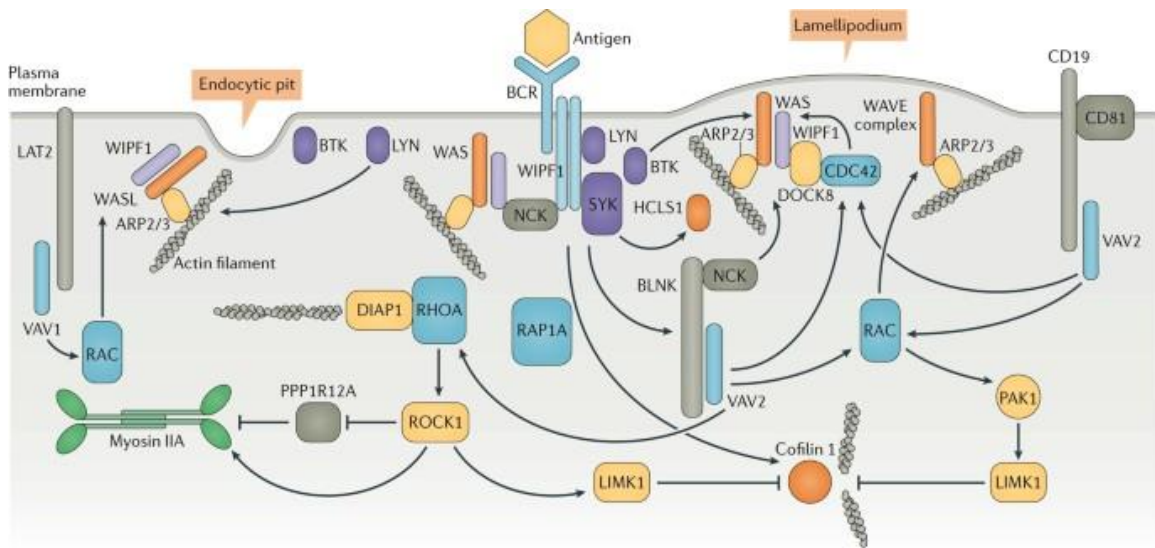
1.3 Lymphoid Tumor Microenvironment

B cell lymphomas depend on and interact with their lymphoid tumor microenvironment (Ly-TME), which includes immune cells, stromal cells, extracellular matrix (ECM) and blood vessels [13]. Key Ly-TME components in DLBCL include T cell subsets (CD4⁺ T cells), macrophages, endothelial cells, and the ECM [13]. CD4⁺ T cells express CD40L, a type II transmembrane protein with a molecular weight between 32-39 kDa, which interacts with CD40 expressed on B cells and induces B cell activation and proliferation. CD40-CD40L engagement induces the clustering of CD40 and recruitment of TNFR-associated factors (TRAFs) to CD40 cytoplasmic domains, which can activate canonical and non-canonical NF- κ B signaling [14]. TRAF6 is recruited to the cytoplasmic domains of CD40 upon CD40-CD40L engagement and is involved in the formation of the MYD88-TLR9-BCR super complex, suggesting an intersection of both pathways that could contribute to NF- κ B signaling. However, the impact of CD40-CD40L engagement on BCR signaling in ABC DLBCL has not been elucidated.

Tumor cell survival and signaling have also been shown to depend on the interaction between stiffness of the lymphoid tissue ECM and integrins expressed on lymphoma cells. Signaling mediators such as Bruton's tyrosine kinase (BTK), mitogen-activated protein kinases (MAPKs), and AKT intersect with integrin α 4 β 1 expressed on DLBCLs [15-17]. In lymphoid follicles, follicular dendritic cells (FDCs) express vascular cell adhesion molecule (VCAM)-1 [19] which binds to α 4 β 1. Previous work has shown that organoid stiffness impacts the proliferation of ABC DLBCL and differentially regulates integrin β 1 expression [18]. The impact of CD40-CD40L engagement on ABC DLBCL BCR activation and signaling however has not been investigated.

1.4 B Cell Receptor Signaling and the Actin Cytoskeleton Coordination

Binding of antigen to the BCR triggers cortical cytoskeleton remodeling, which drives B cell spreading and adhesion on the antigen-bound surface, and facilitates immune synapse formation (between B cells and APCs), followed by extraction and endocytosis of antigen [20]. The cortical cytoskeleton consists of a meshwork of actin filaments attached to the plasma membrane, the dynamics of which are controlled by actin nucleation factors (actin related protein 2/3 [ARP2/3] and formins), severing proteins (cofilin 1 and destrin), debranching proteins (coronins), and capping proteins (e.g., capping actin protein [CAPZA]). In the BCR signaling pathway, phosphorylation of BCR, B cell linker protein (BLNK), CD19 and linker for activation of T cell family member 2 (LAT2) activates the Wiskott-Aldrich syndrome family of proteins (WASP) [21,24] and WAS protein family verprolin-homologous protein (WAVE), which induces actin polymerization through the ARP2/3 complex, resulting in the formation of filopodia, lamellipodia or endocytic pits in the plasma membrane (Figure 2) [22,23,25]. Investigating the dynamics of actin cytoskeleton in ABC DLBCL could provide insight into the cytoskeletal reciprocal regulation of BCR signaling and thus help to identify targets in the cortical cytoskeleton for therapeutic interventions.



Nature Reviews | Immunology

Figure 2: B Cell Receptor Signaling and the Actin Cytoskeleton Coordination

1.5 Motivation and Objectives

This research aims to investigate the effects of lymphoid tumor microenvironment cues, specifically CD40L and extracellular matrix stiffness, on B cell receptor signaling in activated B cell-like diffuse large B-cell lymphoma. We use 2D models to recreate membrane bound antigen and 3D models to recreate soluble antigen with the goal of recapitulating native aspects of the Ly-TME and B cell interactions with Ly-TME elements. By examining expression, clustering and colocalization of IgM BCR, CD40, and actin, we aim to investigate the effects of the Ly-TME cues on ABC DLBCL BCR signaling and the intersection of the BCR signaling pathway and CD40-CD40L engagement induced activation of NF-Kb.

CHAPTER 2: METHODS

2.1 Polymer and Peptides

Maleimide functionalized 4-arm polyethylene glycol (PEG-MAL) (20,000 Da, $\geq 90\%$ purity) was purchased from Laysan Bio. Adhesive peptide “REDV” (GREDVGC) and VPM (GCRDVPMS↓MRGGDRCG) with above 95% purity was purchased from AAPPTec. Non degradable crosslinker dithiothreitol (DTT) was purchased from Sigma Aldrich.

2.2 Cell culture

OCI-Ly10 were obtained from Ari Melnick (Weill Cornell Medicine, New York, NY) and were cultured in Iscove’s medium supplemented with 20% Fetal Bovine Serum, 1% Glutamax and 2% penicillin/streptomycin. OCI-LY10 is a human ABC-DLBCL cell line with mutation in CD79A, with WT CARD11 (T Clozel, 2013; Tian et al., 2015)

2.3 DLBCL Lymphoma 2D model preparation

For the 2D model, anti IgM or/and CD40L monolayers were prepared by adding 150 μL of anti IgM only antibody solution (0.5 mg/ml or 3.33 μM), soluble CD40L solution (0.072 mg/ml or 3.33 μM) or anti IgM and CD40L solution (1:1 molar ratio), on glass bottom dishes. The anti IgM or soluble CD40L solutions were adsorbed on glass bottom dishes and were purchased from Fisher Scientific and R&D systems respectively.

OCI-Ly10 (50k cells/100 μ L) were added and incubated at 37 °C in an incubator for 24 hours.

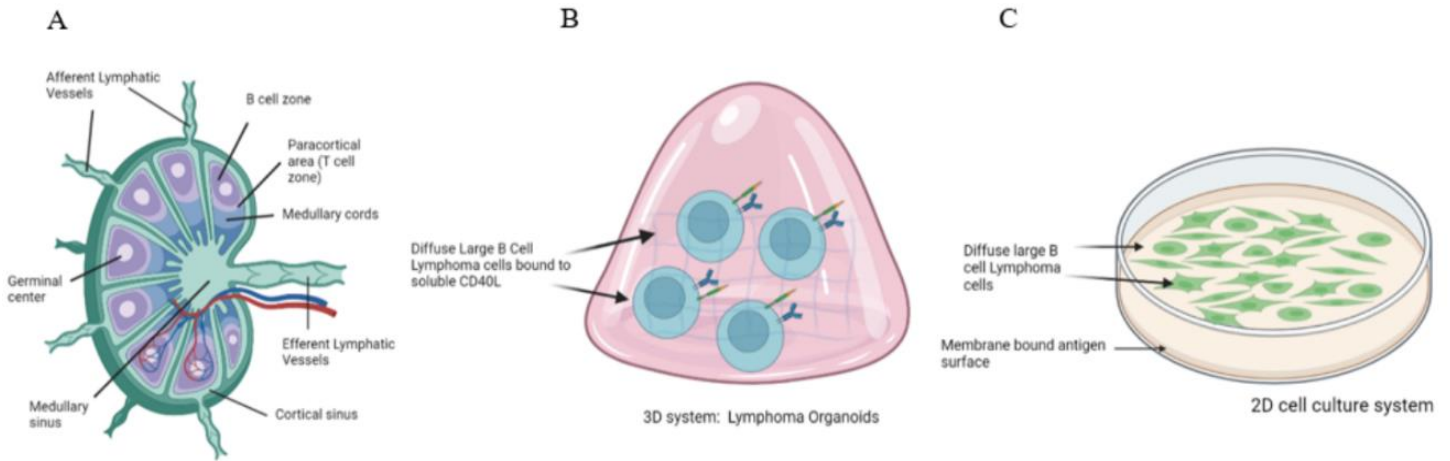


Figure 3: A) Organization of a lymph node. b) Schematic of our 3D model: Lymphoma Organoids. C) Schematic of our 2D model - Antigen/CD40L monolayer. All schematics generated using Biorender.

2.4 2D cell culture immunostaining

After 24 hours, the cells were fixed with 4% of Formaldehyde in 1x DPBS for 10 minutes at room temperature, washed twice with DPBS and permeabilized with 2% Triton X-100 for 10 minutes at room temperature. This was followed by blocking with 10% bovine serum albumin for 30 minutes and another washing step. The samples were then stained with primary antibodies which included rabbit anti human CD40 (1:100 dilution) and mouse anti human IgM (1:100 dilution) and incubated at 4°C overnight.

This was followed by a washing step and staining with secondary antibodies which included donkey anti rabbit Alexa Fluor 488 (1:100 dilution), donkey anti mouse Alexa Fluor 647 (1:100 dilution) and incubation for 1 hour at room temperature. The samples were then washed twice and incubated with phalloidin Alexa fluor 555 for 10

minutes and then DAPI for 10 minutes. DPBS was then added to each dish for long term storage.

2.5 Organoid Fabrication

We engineered synthetic hydrogel organoids that are composed of maleimide functionalized 4-arm polyethylene glycol (PEG-4MAL). The PEG-4MAL macromers were functionalized with integrin $\alpha 4\beta 1$ binding adhesive peptide, “REDV” (GREDVGC) peptide, which mimics Vascular Cell Adhesion Molecule (VCAM)-1, expressed by follicular dendritic cells (FDCs) in B cell follicles (Figure 2). One arm of the PEG-4MAL was functionalized with thiolated short REDV peptides through a Michael -type addition reaction between MAL and thiol groups; PEGMAL macromers were first conjugated with REDV peptides.

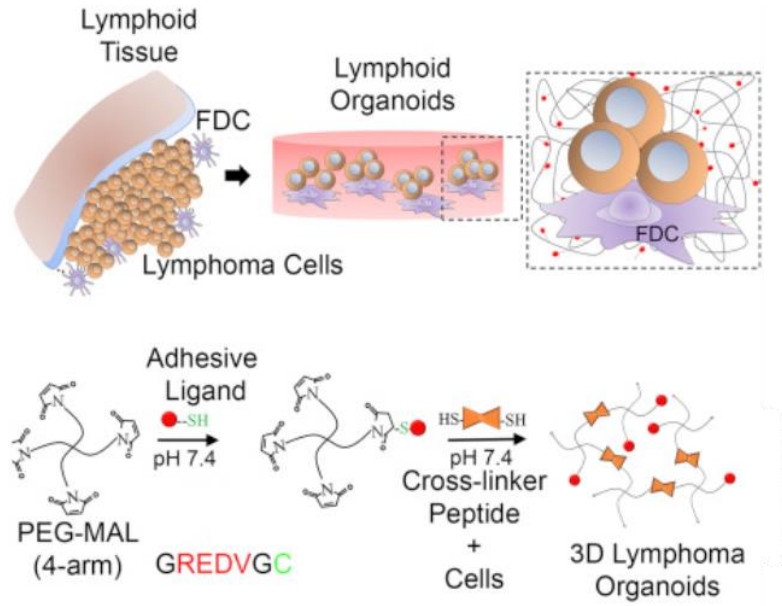


Figure 4: Schematic of lymphoma organoid formation and Michael Addition chemistry; organoids are encapsulated with lymphoma cells and follicular dendritic cells [25].

Degradable crosslinker VPM and non-degradable crosslinker (DDT) was used in a 1:1 ratio to crosslink the hydrogel macromers. DDT was used to regulate hydrogel degradation kinetics and VPM was chosen specifically because of its sensitivity to matrix metalloproteinase (MMP) 9, found in B cell lymphomas. Anti IgM antibody, soluble CD40L or Anti IgM and CD40L were incubated with ABC DLBCLs (OCI-Ly10, 40k cells/organoid) for 10 minutes on ice and were resuspended in the crosslinker solution. After mixing macromers, peptides, cells and crosslinkers, 10 μ L droplets of the mixture were placed in 24 well plates and cured for 15 minutes at 37 °C in an incubator prior to adding media.

2.6 Organoid Immunostaining for Imaging

After 24 hours, the organoids were fixed with 4% paraformaldehyde in PBS for 2 hours at room temperature, washed twice, permeabilized with 0.5% Triton X-100 in PBS for 30 minutes at room temperature and washed twice again. This was followed by a blocking step with normal donkey serum for 30 minutes at room temperature and then the primary antibodies which included rabbit anti human CD40 (1:100 dilution) and mouse anti human IgM (1:100 dilution) were added and incubated at 4 °C overnight.

After overnight incubation, the organoids were washed twice with PBS and stained with secondary antibodies which included donkey anti rabbit Alexa Fluor 488 (1:100 dilution), donkey anti mouse Alexa Fluor 647 (1:100 dilution), phalloidin Alexa Fluor 555(1:50 dilution) and DAPI (1:1000 dilution) in the dark for 4 hours. Samples were then washed and stored in PBS at 4 °C.

2.7 Confocal Imaging and Image analysis

Z stacks of single cells on the 2D monolayers and encapsulated in organoids were imaged and obtained using Zeiss Laser Scanning Confocal Microscope. Channels 488, 647, 555 and 405 were chosen using the smart setup option and the intensity and gain values were kept constant within each stiffness or 2D group. Maximum intensity projections of each single cell image file were done to quantify and analyze area, mean fluorescence intensity, cluster number etc.

2.8 Statistical analysis

GraphPad Prism software was used to perform 1-way and 2- way Analysis of Variance (ANOVA). A p-value of less than 0.05 was considered significant. 20 single cell images were taken per condition and outliers were removed using the ROUT outliers' tool. All values are reported as Mean \pm S.E.M.

CHAPTER 3: RESULTS

3.1 Comparison of different modes of antigen presentation in 2D and 3D ABD DLBCL models

B cells encounter antigen, differentiate into plasmablasts, plasma cells or memory B cells and contribute to the induction of the adaptive immune response in specialized secondary lymphoid organs such as the lymph node (Figure 3A). There are multiple modes for antigen encounter of B cells in B cell follicles, sub anatomical structures in lymph nodes, with either soluble antigen or membrane bound antigens - antigen processed and presented by antigen presenting cells (APCs). To recapitulate the in vivo lymphoid tumor microenvironment (Figure 3A, 5A) and the cellular and biophysical cues necessary for ABC DLBCL activation and signaling, we engineered 2D and 3D models.

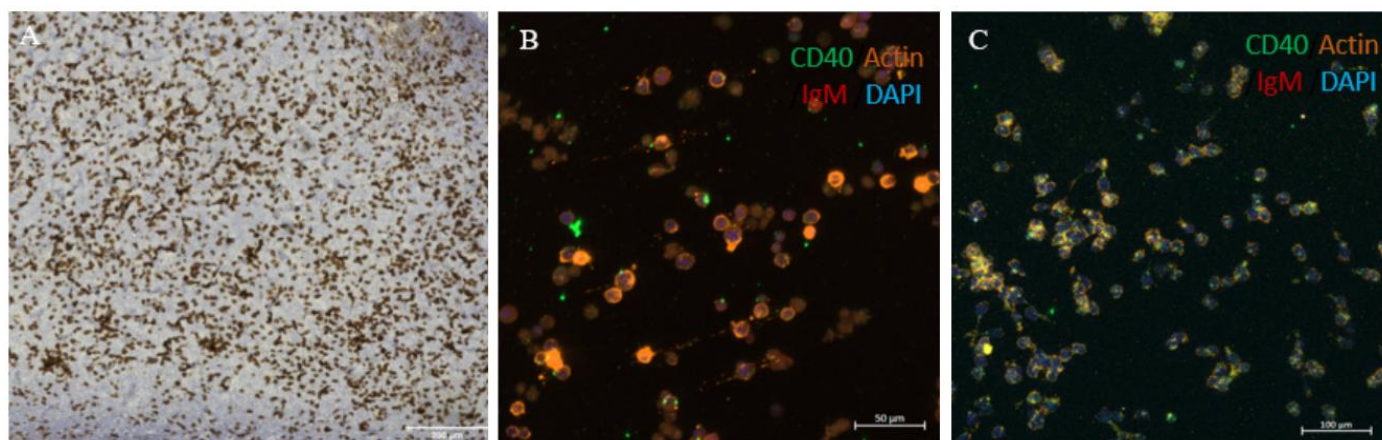


Figure 5: A) T cells within patient ABC-DLBCL biopsy specimen. Brown = CD3 (Provided by Dr. Jean Koff). B) Ly10 cells encapsulated in 7.5 wt% /vol oragnoids. (3D model) C) Ly10 cells spreading on 2D monolayer (2D model)

In the 2D model (Figure 3C, 5C), the presentation of antigen on the surfaces of lymph node APCs was simulated to investigate the effects of CD40-CD40L interaction on BCR signaling. 2D monolayers composed of Anti IgM antibody, CD40 ligand, and

Anti IgM and CD40 ligand (1:1 molar ratio) were prepared and ABC DLBCLs were seeded and exposed to the layers for 24 hours. In the 3D model (Figure 3B, 5B), Anti IgM antibody or/and soluble CD40L was encapsulated in the organoids of varying PEG-4-MAL wt%/vol and the cells were exposed to Anti IgM and/or CD40L for 24 hours as well.

3.2 Investigating CD40-CD40L effects on DLBCL BCR signaling in 2D vs 3D model

DLBCL cell morphology was observed to be different in 2D and 3D models (Figure 6), where majority of the cells in the 2D model were observed to have distinct filapodia structures compared to the cells in the organoids; approximately 55% of cells exhibited filapodia when exposed to Anti IgM and CD40L (Figure 6, 7A). ABC DLBCL cell spreading was greater with membrane bound antigen and/or CD40L presentation in the 2D model compared to soluble antigen and/or CD40L presentation in the organoids

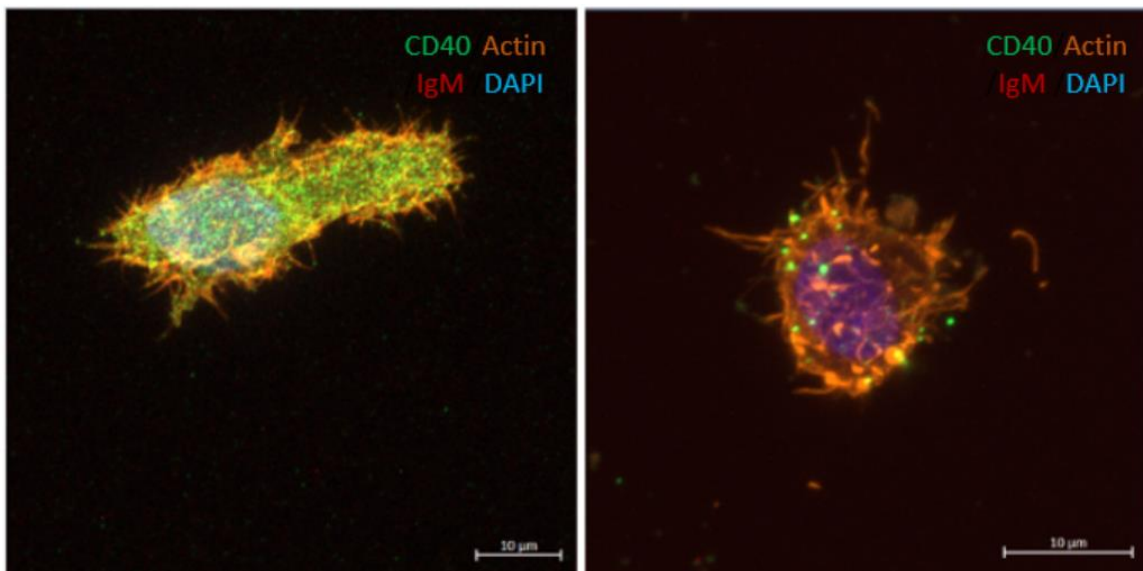


Figure 6: Cell spreading and filapodia formation in 2D cell culture (L) and 7.5 wt%/vol organoids (R).

(Figure 6, 7B), where cell spreading area was 393.4 μm^2 in the 2D model with Anti IgM and CD40L exposure and was 141.6 μm^2 in the organoids.

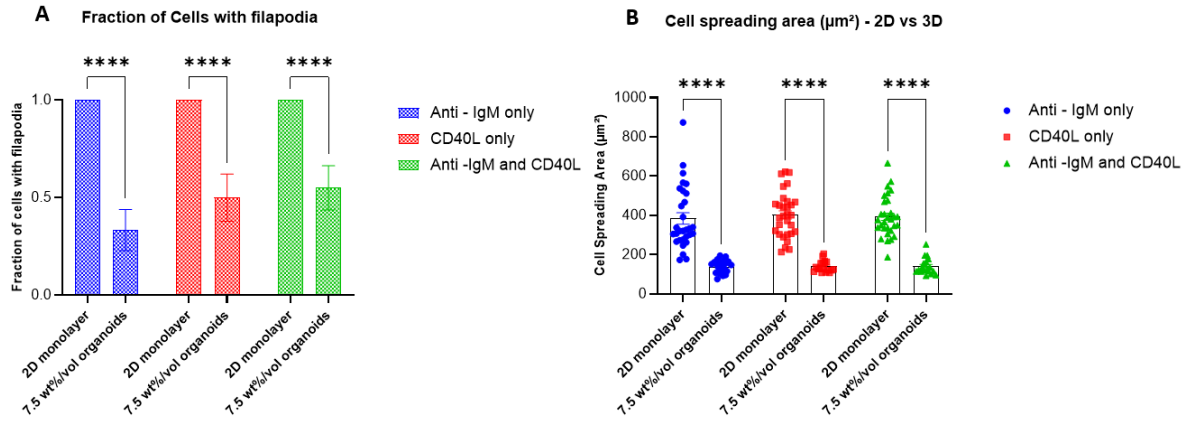


Figure 7: A) Comparing fraction of cells with filapodia in 2D vs 3D. B) Comparing cell spreading area in 2D vs 3D

Distinct CD40 clusters were formed in cells encapsulated in the organoids compared to cells in the 2D system, where CD40 was spread across the cell membrane, and the normalized CD40 mean fluorescence intensity was significantly lower in the 7.5 wt%/vol organoids compared to the 2D model (Figure 6). The normalized actin and CD40 MFI values were generated by normalizing actin and CD40 MFI values for both groups with the mean anti IgM MFI value for 2D and 7.5 wt%/vol organoids respectively. In the 7.5 wt%/vol organoids, normalized CD40 MFI was significantly lower when cells were presented with both Anti IgM and CD40L, compared to only antigen presentation (Figure 8B). However, there was no significant difference in actin expression and between the 2D or 3D models (Figure 8A) and no significant difference between antigen and CD40L presentation and antigen presentation only.

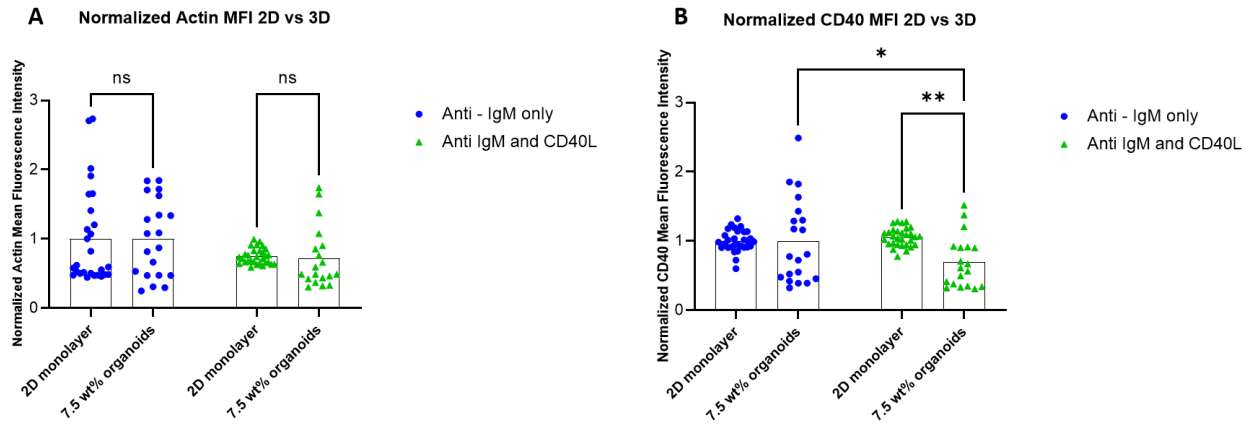


Figure 8: Comparing Actin expression (A) and CD40 expression (B) in 2D vs 3D

3.3 Investigating CD40-CD40L effects on DLBCL BCR signaling in 3D model

By replicating aspects of the native lymphoid microenvironment to provide spatiotemporal control of biomolecular and biophysical cues that 2D cultures cannot provide, organoids with varying PEG-4-MAL wt%/vol were synthesized, to eventually investigate the effects of CD40-CD40L interaction on ABC DLBCL signaling as well as the effects of ECM stiffness on ABC DLBCL BCR signaling in a 3D model. The storage modulus for each wt%/vol was obtained by previous rheology characterization studies and was observed to increase with increasing wt%/vol; 7.5 wt%/vol, 10 wt%/vol and 12.5 wt%/vol PEG-4-MAL organoids had a storage modulus of 537.4 Pa, 571.71 Pa and 1452.62 Pa respectively (Figure 9).

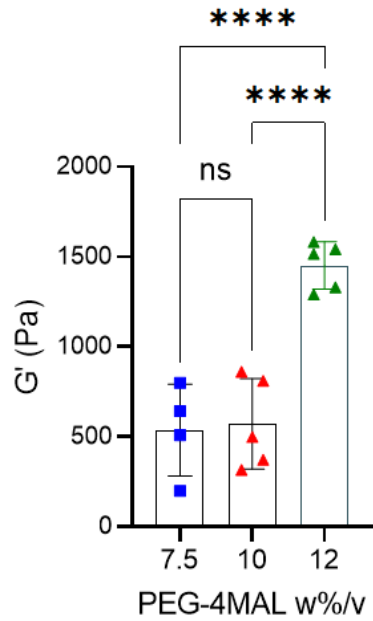


Figure 9: Stiffness versus PEG-4MAL wt%/v

3.3.1 Actin expression and cell spreading with antigen and CD40L presentation in 3D model

By analyzing actin expression among the three antigen/CD40L presentation groups, CD40L is observed to reduce actin expression in the 10 wt%/vol and 12.5 wt%/vol organoids. (Figure 10)

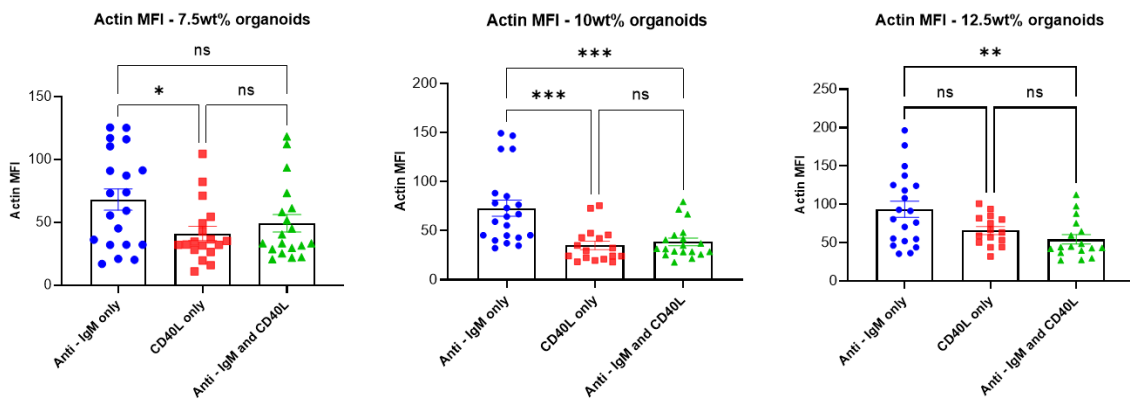


Figure 10: Comparing Actin MFI across three anti IgM/CD40L groups for each wt%/vol condition

Cell spreading area did not vary upon anti IgM and/or CD40L presentation in the 7.5wt%/vol and 10 wt%/vol organoids. However, in the 12.5 wt%/vol organoids, CD40L presentation reduced cell spreading significantly, where cell spreading area was recorded to be 129.4 μm^2 upon Anti IgM presentation only and 100.2 μm^2 for Anti IgM and CD40L presentation (Figure 11).

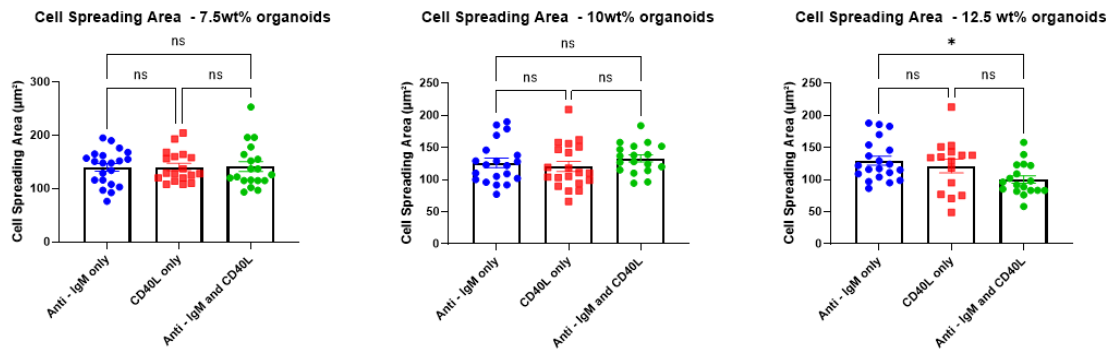


Figure 11: Comparing Cell spreading MFI across three anti IgM/CD40L groups for each wt%/vol condition

To analyze actin expression across all three stiffness conditions and investigate the effects of Ly-TME stiffness on ABC DLBCL actin expression, we generated normalized actin MFI values by normalizing actin MFI values in the Anti IgM and CD40L condition to the mean Anti IgM MFI value for each stiffness condition. However, we did not observe any significant difference in actin expression with varying stiffness (Figure 12A). Cell spreading area was observed to decrease with increasing stiffness upon anti IgM and CD40L presentation, where mean cell spreading area was measured to be 141.6 μm^2 and 100.2 μm^2 in the 7.5 wt%/vol organoids and 12.5 wt%/vol organoids respectively (Figure 12B). This suggest that in stiffer organoid conditions and CD40-CD40L engagement, the cells are in the antigen extraction and endocytosis stage

mediated by actin myosin contractility and BCR clustering, resulting in reduced actin polymerization and cell spreading.

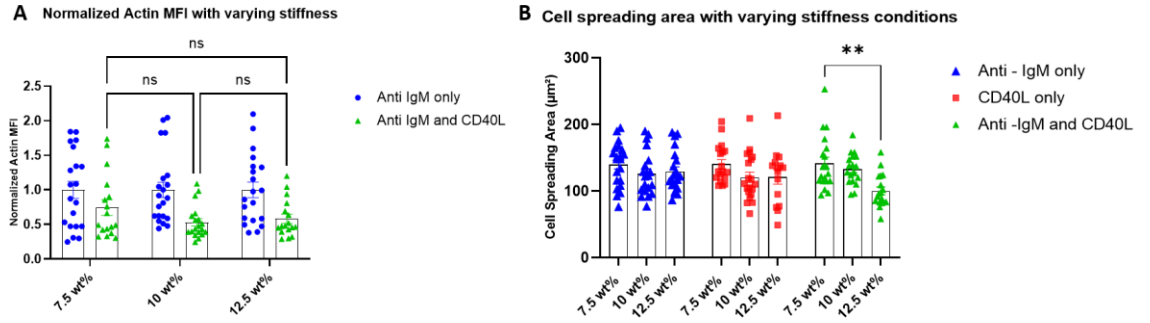


Figure 12: A) Comparing normalized actin MFI with varying stiffness B) Comparing cell spreading area with varying stiffness

3.3.2 CD40 cluster and expression with antigen and CD40L presentation in 3D model

To investigate the CD40-CD40L interaction with varying antigen/CD40L presentation and stiffness, CD40 clusters were quantified and the CD40 expression was analyzed for each cell. When comparing CD40 cluster number across the three groups of anti-IgM and CD40L presentation, CD40 cluster number only varied significantly between the Anti IgM only and CD40L only groups, where mean CD40 cluster number was quantified to be 26.4 and 40.35 when cells were presented with anti-IgM only and CD40L only respectively in the 7.5 wt%/vol organoids. No significant difference in CD40 cluster number was observed between all three groups in the 10wt%/vol and 12.5

wt%/vol organoids (Figure 13).

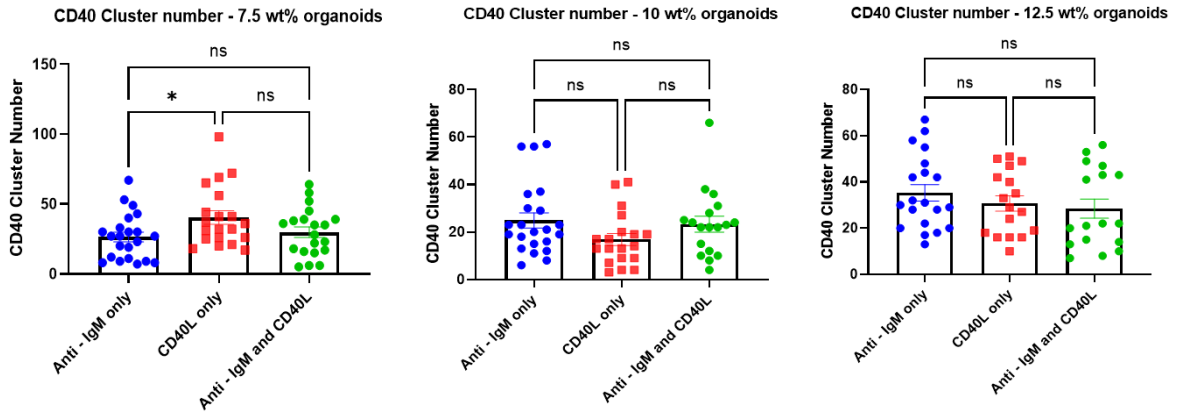


Figure 13: Comparing CD40 cluster number across three anti IgM/CD40L groups for each wt%/vol condition

No significant difference was observed in CD40 mean fluorescence intensity across the three groups in all the 7.5 wt%/vol and 10 wt%/vol organoids, however in the 12.5 wt%/vol organoids, CD40 MFI was reported to be greater in cells exposed to antigen and CD40L compared to cells only exposed to CD40L; CD40 MFI for CD40L only and anti - IgM and CD40L group was 36.8 and 55.36 respectively (Figure 14).

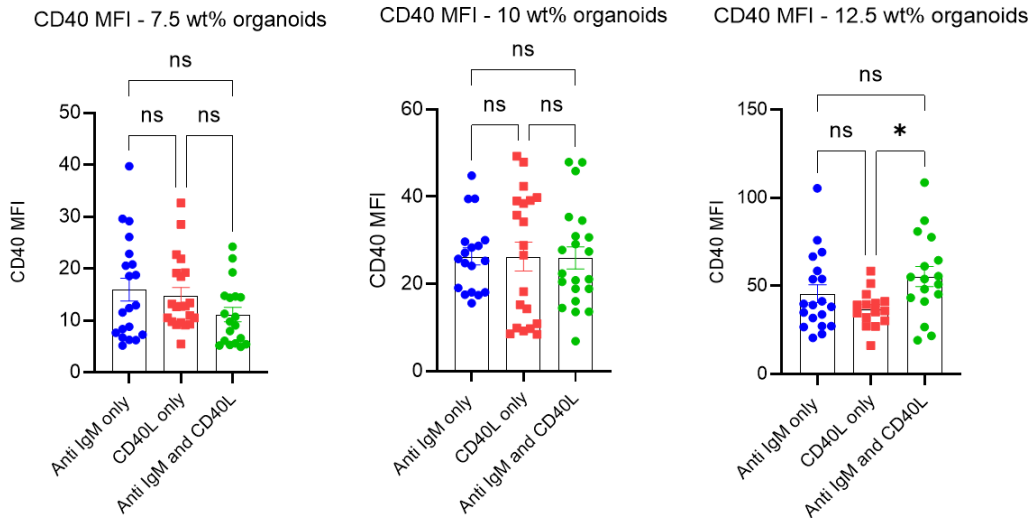


Figure 14: Comparing CD40 MFI across three anti IgM/CD40L groups for each wt%/vol condition

To assess the impact of Ly-TME stiffness on CD40 expression and CD40 Cluster number, normalized CD40 MFI values were generated by normalizing all CD40 MFI values from anti IgM only group and anti IgM and CD40L group with the average CD40 MFI value of the Anti IgM group for each stiffness condition.

Normalized CD40 MFI and CD40 expression only varied between the 7.5wt%/vol (0.7 normalized CD40 MFI) and 12.5 wt%/vol (1.2 normalized CD40 MFI), where CD40 expression increased with increasing stiffness (Figure 15A). CD40 cluster numbers only varied between the 7.5 wt%/vol (40.35) and 10wt%/vol (16.84) organoids (Figure 15B).

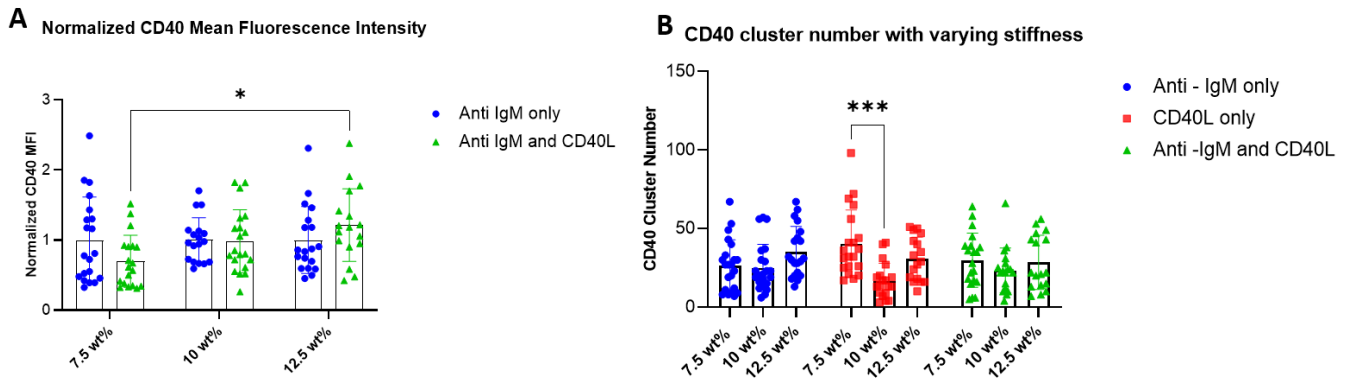


Figure 15: A) Comparing normalized CD40 MFI with varying stiffness. B) Comparing CD40 cluster number with varying stiffness

3.3.3 BCR clustering and expression with antigen and CD40L presentation in 3D model

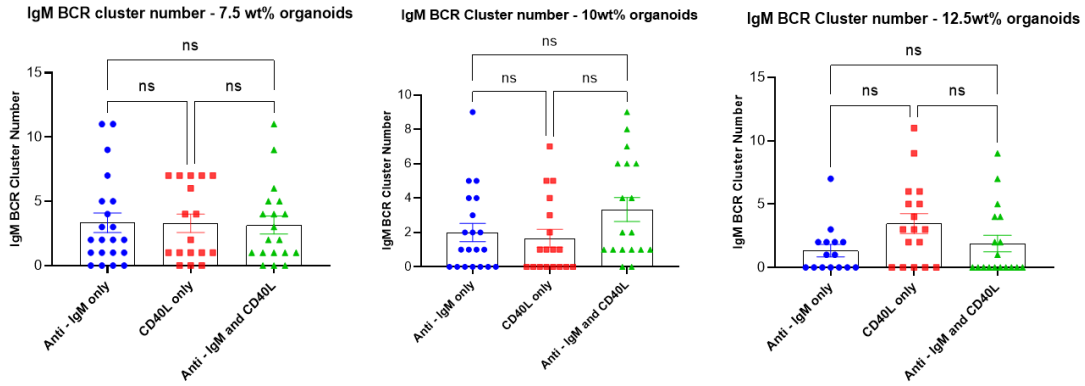


Figure 16: Comparing IgM BCR Cluster number across three anti IgM/CD40L groups for each wt%/vol

To investigate BCR clustering and expression with varying antigen/CD40L presentation and Ly-TME stiffness, BCR clusters were quantified for each cell after antigen/CD40L presentation for 24 hours and the normalized IgM BCR MFI values were generated. No significant difference was observed in the IgM BCR cluster number and BCR MFI by varying antigen/CD40L presentation groups (Figure 16, 17).

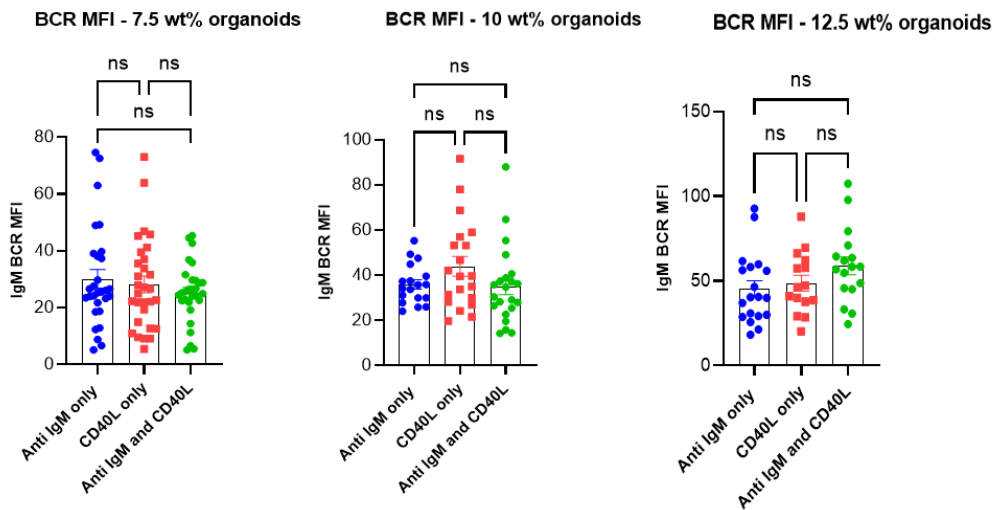


Figure 17: Comparing IgM BCR MFI across three anti IgM/CD40L groups for each wt%/vol condition

Normalized IgM BCR MFI varied between 7.5 wt%/vol (0.81) and 12.5 wt%/vol (1.3) organoids, where IgM BCR increased with increasing stiffness in cells presented with Anti IgM and CD40L (Figure 18A). However, no significant difference was observed in BCR cluster number across the three stiffness conditions (Figure 18B).

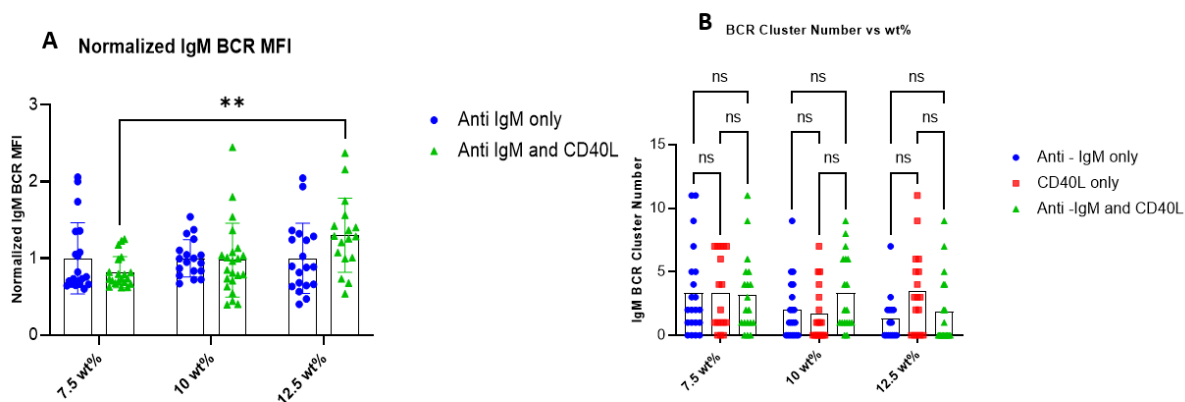


Figure 18: A) Comparing normalized IgM BCR MFI with varying stiffness. B) Comparing BCR Cluster number with varying stiffness

3.3.4 Colocalization analysis of IgM BCR, Actin and CD40

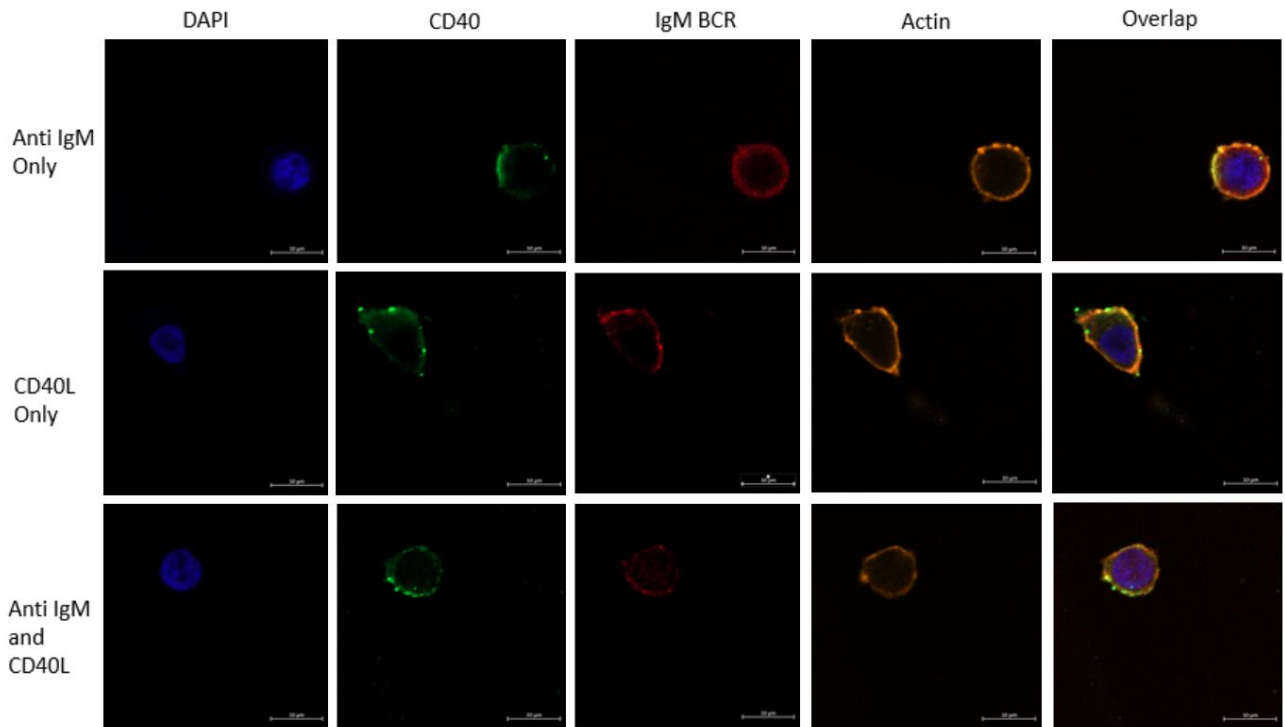


Figure 19: IgM BCR and CD40 cluster colocalization and Actin and CD40 colocalization observed in 12.5 wt%/vol organoids

To further investigate CD40-CD40L interaction on BCR signaling, the colocalization or spatial overlap of IgM BCR and CD40 was analyzed and reported as the Manders Colocalization Coefficient for each cell. While the colocalization of IgM BCR and CD40 did not vary by changing presentation of antigen/CD40L, it significantly increased with increasing stiffness conditions in all three presentation groups. In cells presented with anti-IgM only, the colocalization coefficient increased from 0.75 to 0.85 as the PEG-4-MAL wt% increased from 7.5 wt%/vol to 12.5 wt%/vol. In cells presented with CD40L only, the colocalization coefficient increased from 0.77 to 0.84 as the PEG-4-MAL wt% increased from 7.5 wt%/vol to 12.5 wt%/vol. And finally, in cells exposed

to anti IgM and CD40L, the colocalization coefficient was 0.77, 0.8 and 0.86 for the 7.5wt%/vol, 10 wt%/vol and 12.5 wt%/vol organoids (Figure 19).

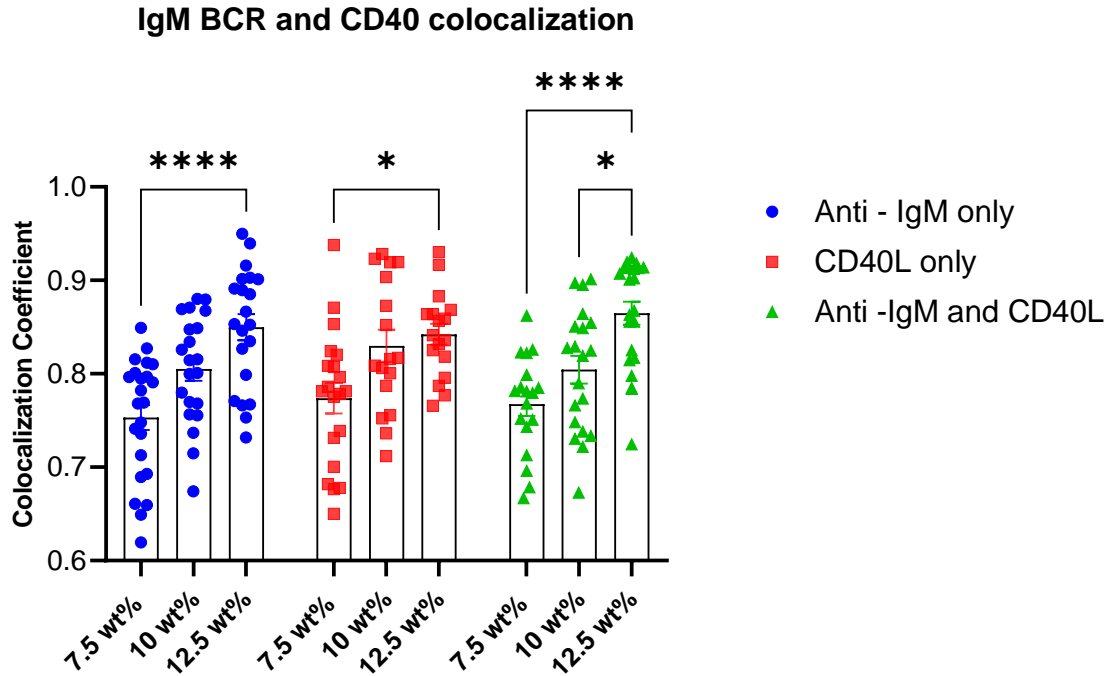


Figure 20: IgM BCR and CD40 colocalization. Each point represents the average mander's overlap coefficient for each stack of an entire image file.

Similar analysis was done to determine the colocalization of CD40 and Actin, which was reported to increase with increasing stiffness as well but did not vary in antigen/CD40L presentation groups. In cells exposed to anti IgM, the colocalization coefficient was 0.67, 0.76 and 0.80 for the 7.5wt%/vol, 10 wt%/vol and 12.5 wt%/vol organoids. In cells exposed to CD40L, the colocalization coefficient was 0.7, 0.8 and 0.8 for the 7.5wt%/vol, 10 wt%/vol and 12.5 wt%/vol organoids. And finally, in cells exposed to anti IgM and CD40L, the colocalization coefficient was 0.7, 0.73 and 0.84 for the 7.5wt%/vol, 10 wt%/vol and 12.5 wt%/vol organoids. These results demonstrate a significant effect of the Ly-TME stiffness environment on the spatiotemporal relationship

between IgM BCR and CD40 and Actin and CD40 (Figure 20) and potential involvement mechanotransduction pathways mediated by integrin expression in the colocalization.

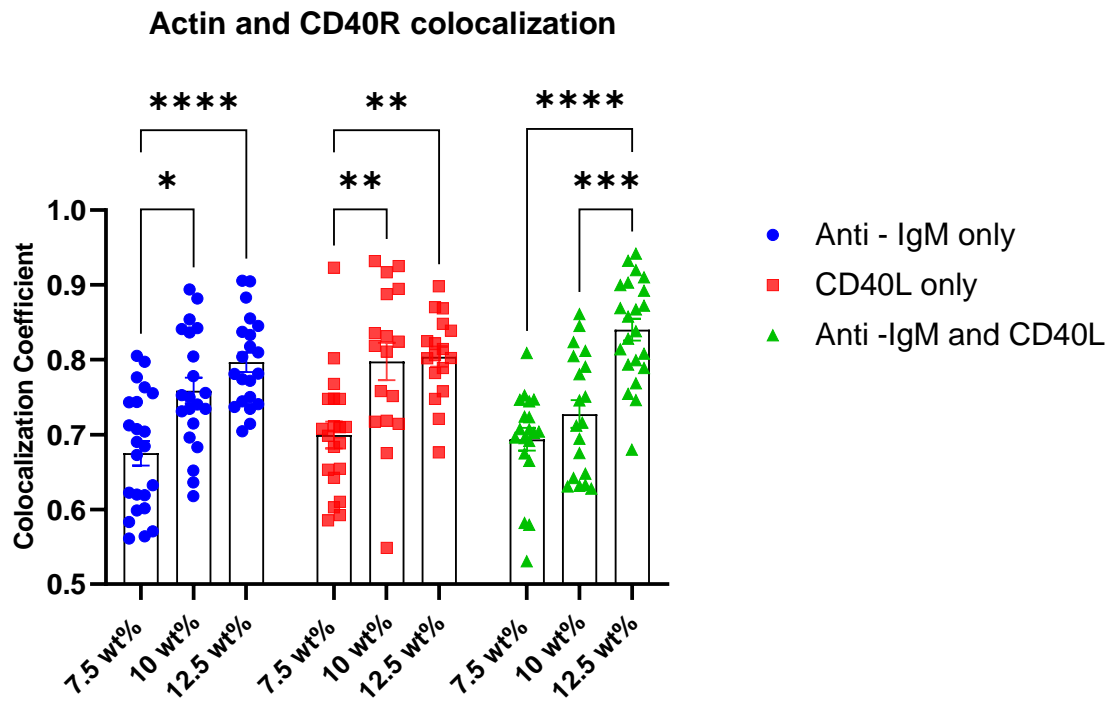


Figure 21: Actin and CD40 colocalization. Each point represents the average mander's overlap coefficient for each stack of an entire image file

CHAPTER 4: DISCUSSION

To investigate the effects of Ly- TME cues, specifically CD4+ T cell signaling via CD40L and the stiffness of the ECM on ABC DLBCL BCR signaling, we engineered 2D and 3D models. With our 2D model, we aimed to recapitulate B cell encounter of membrane bound antigen, where the B cells would spread over the surface containing adsorbed antigen, would gather antigen through their BCRs forming clusters and immune synapses, mimicking the response of B cells to antigen presented by antigen presenting cells. Our 3D model comprises of lymphoma organoids, synthetic PEG-4MAL hydrogels that recapitulates several biophysical and molecular Ly-TME cues and B cell encounter of soluble antigen by encapsulating DLBCLs and soluble anti IgM and CD40L.

DLBCL B cell spreading and filapodia formation was observed in both the 2D layers and the organoids, which indicates enhanced actin remodeling, activation of WAS and WAVE family of proteins and the ARP2/3 complex which induces actin polymerization and filapodia formation [20,21,23,25]. Cell spreading and filapodia formation was significantly greater in the 2D layers, however they do not provide a realistic replication of the spatial temporal control of Ly-TME cues that our organoids aim to recapitulate.

We varied PEG-4MAL wt%/vol to prepare organoids with three different stiffness conditions to investigate the effects of ECM stiffness on BCR signaling as previous studies have shown that DLBCLs proliferate differentially in different stiffness environments which modulates integrin expression, BCR signaling and response to therapeutics [18]. We observed reduced actin expression and cell spreading upon CD40L

presentation in our stiffer organoids (10 wt%/vol and 12.5 wt% vol) and reduced cell spreading with increasing stiffness, suggesting that in stiffer Ly-TME, cells with BCR and CD40-CD40L engagement are in the antigen extraction and endocytosis stage and B cell spreading has ceased.

CD40-CD40L engagement results in CD40 clustering and recruitment of TRAFs to the CD40 cytoplasmic domains that eventually activates canonical and non-canonical NF-B signaling [14]. We only observed significant increase in CD40 expression in the stiffer organoids (12.5 wt%/vol) with BCR engagement (Anti IgM and CD40L) compared to no BCR engagement (CD40L only), suggesting that cells with antigen bound BCR and CD40-CD40L engagement showed increased CD40 expression compared to cells without antigen bound BCR, however there was no difference in CD40 cluster number. CD40 expression did increase with increasing stiffness when cells were exposed to both antigen and CD40L.

Also, CD40-CD40L engagement induced CD40 clustering increased as stiffness increased from 7.5wt%/vol to 10wt%/vol but did not significantly vary with the 12.5 wt% groups. Our results suggest that in stiffer Ly-TME, increased CD40 expression and reduced number of CD40 clusters are observed however we need to investigate this by increasing our antigen exposure time point to 24 hours to verify this.

BCR clustering and expression did not significantly vary by antigen and/or CD40L presentation, however IgM BCR expression with CD40-CD40L engagement was enhanced in stiffer organoids, where BCR expression increased with increasing stiffness i.e., from 7.5wt%/vol to 12/5 wt%/vol. We did not observe any differences in BCR

cluster number with stiffness and CD40L; further investigation will be done as a part of our future experiments at increased time points to verify our findings.

Our colocalization analysis data suggests a significant impact of lymphoid TME on the spatiotemporal relationship between IgM BCR and CD40 as well as Actin and CD40.

Increased colocalization between IgM BCR and CD40 and Actin and CD40 was observed with increasing stiffness, from 7.5 wt%/vol to 12.5 wt%/vol, with maximum

spatiotemporal overlap at 12.5 wt%/vol. This suggests that matrix stiffness could be generating mechanical cues that promotes integrin stimulation or other

mechanotransduction pathways [15-17] to engage CD40L with Actin or IgM BCR.

Further investigation will help elucidate the intersection of CD40-CD40L engagement in stimulating mechanotransduction pathways and ultimately downstream BCR signaling.

CHAPTER 6: CONCLUSION AND FUTURE DIRECTIONS:

We aimed to elucidate the effects of CD40L and ECM stiffness on ABC DLBCL BCR signaling and provide preliminary data for further investigation, through 2D and 3D platforms. In our 2D platform, we recapitulated membrane bound antigen B cell encounter and activation and observed significant cell spreading and filopodia formation compared to soluble antigen presentation in our organoids. In our 3D organoids, we observed a significant decrease in actin expression and cell spreading with increasing stiffness. CD40 and IgM BCR expression increased as stiffness of the organoids increased from the 7.5wt%/vol organoids to the 12.5 wt%/vol organoids, however IgM BCR cluster number did not vary with stiffness and CD40 cluster number varied between the 7.5 wt%/vol and the 10 wt%/vol organoids. We observed significant impact of stiffness on IgM BCR and CD40 colocalization and CD40 and Actin colocalization, suggesting the involvement of the lymphoid microenvironment in stimulating mechanotransduction pathways to colocalize IgM and CD40 or IgM and actin. Further investigation into BCR and CD40 clustering and expression will be done at increased time points (48-hour time points) to verify our current results. To perform an in dept analysis of interaction between CD40-CD40L with IgM BCR signaling, the proximity ligation assay (PLA) will be used to identify adapter proteins or kinases in the ABC DLBCL BCR signaling pathway such as BTK, MALT1, CBM complex, MYD88, TLR9 etc. that are in proximity with CD40. High resolution microscopy techniques such as Direct stochastic optical reconstruction microscopy (DSTORM) will be used to quantify and analyze specific BCR and CD40 clusters and measure area, volume, number etc.

REFERENCES

1. SEER P. Surveillance Epidemiology and End Results wwwseercancer.gov.2002.
2. Swerdlow SH, Campo E, Pileri SA, et al. The 2016 revision of the World Health Organization classification of lymphoid neoplasms. *Blood* 2016; 127:2375–2390.
3. Phelan, J.D. et al. A multiprotein supercomplex controlling oncogenic signaling in lymphoma. *Nature* (2018).
4. Chapuy, B. et al. Molecular subtypes of diffuse large B cell lymphoma are associated with distinct pathogenic mechanisms and outcomes. *Nat Med* 24, 679-690 (2018).
5. Roschewski, M., Staudt, L.M. & Wilson, W.H. Diffuse large B-cell lymphoma-treatment approaches in the molecular era. *Nat Rev Clin Oncol* 11, 12-23 (2014).
6. Reth M Antigen receptor tail clue. *Nature* 1989;338:383–384.
7. Saijo K, Schmedt C, Su IH, et al. Essential role of Src-family protein tyrosine kinases in NF-kappaB activation during B cell development. *Nat Immunol* 2003;4:274–279.
8. Turner M, Schweighoffer E, Colucci F, Di Santo JP, Tybulewicz VL. Tyrosine kinase SYK: essential functions for immunoreceptor signalling. *Immunol Today* 2000;21:148–154.
9. Dal Porto JM, Gauld SB, Merrell KT, Mills D, Pugh-Bernard AE, Cambier J. B cell antigen receptor signaling 101. *Mol Immunol* 2004;41:599–613.
10. Davis RE, Brown KD, Siebenlist U, Staudt LM. Constitutive nuclear factor kappa B activity is required for survival of activated B Cell-like diffuse large B cell lymphoma cells. *J Exp Med* 2001;194:1861–1874.
11. Davis RE, Ngo VN, Lenz G, et al. Chronic active B-cell-receptor signalling in diffuse large B-cell lymphoma. *Nature* 2010;463:88–92.

12. Ngo VN, Young RM, Schmitz R, et al. Oncogenically active MYD88 mutations in human lymphoma. *Nature* 2011;470:115–119.
13. Scott, D.W. & Gascoyne, R.D. The tumour microenvironment in B cell lymphomas. *Nat*
14. Elgueta, R. et al. Molecular mechanism and function of CD40/CD40L engagement in the immune system. *Immunol Rev* 229, 152-172 (2009).
15. Dumbauld DW, Lee TT, Singh A, Scrimgeour J, Gersbach CA, Zamir EA, Fu J, Chen CS, Curtis JE, Craig SW, Garcia AJ. How vinculin regulates force transmission, *Proc Natl Acad Sci U S A* 2013;110:9788–93.56.
16. Singh A, Suri S, Lee T, Chilton JM, Cooke MT, Chen W, Fu J, Stice SL, Lu H, McDevitt TC, Garcia AJ. Adhesion strength-based, label-free isolation of human pluripotent stem cells, *Nat Methods* 2013;10:438–44.57.
17. Puklin-Faucher E, Sheetz MP. The mechanical integrin cycle, *J Cell Sci* 2009;122:179–86.
18. Apoorva FNU, Tian YF, Pierpont TM, Bassen DM, Cerchiotti L, Butcher JT, Weiss RS, Singh A. Lymph node stiffness-mimicking hydrogels regulate human B-cell lymphoma growth and cell surface receptor expression in a molecular subtype-specific manner. *J Biomed Mater Res A*. 2017 Jul;105(7):1833-1844.
19. G Rodda, L.B. et al. Single-Cell RNA Sequencing of Lymph Node Stromal Cells Reveals Niche-Associated Heterogeneity. *Immunity* 48, 1014-1028 e1016 (2018).
20. Young, R. M., Phelan, J. D., Wilson, W. H., & Staudt, L. M. (2019) Cytoskeletal control of B cell responses to antigens. *Immunological reviews*, 291(1), 190–213

21. Thrasher, A. J. & Burns, S. O. WASP: a key immunological multitasker. *Nat. Rev. Immunol.* 10, 182–192 (2010).
22. Campellone, K. G. & Welch, M. D. A nucleator arms race: cellular control of actin assembly. *Nat. Rev. Mol. Cell Biol.* 11, 237–251 (2010).
23. Haviv, L. et al. Reconstitution of the transition from lamellipodium to filopodium in a membrane-free system. *Proc. Natl Acad. Sci. USA* 103, 4906–4911 (2006).
24. Keppler, S. J. et al. Wiskott–Aldrich syndrome interacting protein deficiency uncovers the role of the co-receptor CD19 as a generic hub for PI3 kinase signaling in B cells. *Immunity* 43, 660–673 (2015).
25. Rotty, J. D., Wu, C. & Bear, J. E. New insights into the regulation and cellular functions of the ARP2/3 complex. *Nat. Rev. Mol. Cell Biol.* 14, 7–12 (2012).
26. Tian YF, Ahn H, Schneider RS, Yang SN, Roman-Gonzalez L, Melnick AM, Cerchietti L, Singh A. Integrin-specific hydrogels as adaptable tumor organoids for malignant B and T cells, *Biomaterials* 2015;73:110–119.